J Appl Electrochem (2007) 37:1399–1411
DOI 10.1007/s10800-007-9348-7

ORIGINAL PAPER

Carbon supported Ru–Se as methanol tolerant catalysts for DMFC cathodes. Part II: preparation and characterization of MEAs

K. Wippermann · B. Richter · K. Klafki · J. Mergel · G. Zehl · I. Dorbandt · P. Bogdanoff · S. Fiechter · S. Kaytakoglu

Received: 6 November 2006 / Revised: 14 March 2007 / Accepted: 16 March 2007 / Published online: 29 June 2007

Abstract Cathode catalyst layers were prepared and characterized as part of membrane electrode assemblies (MEA) and catalyst coated membranes (CCM) on the basis of carbon supported methanol tolerant $RuSe_x$ catalysts. Preparation parameters varied were: catalyst loading (0.5–2 mg $RuSe_x$ cm^{-2}), PTFE content (0, 6, 18 wt.%), carbon support (Vulcan XC 72 or BP2000), and fraction of $RuSe_x$ in the carbon supported catalysts (20, 44, 47 wt.%). The MEAs and cathode catalyst layers were electrochemically characterized under Direct Methanol Fuel Cell (DMFC) operating conditions by recording polarization curves, galvanostatic measurements, and impedance spectra. The morphology of the catalyst layers was investigated by means of confocal laser scan microscopy (CLSM), scanning electron microscopy (SEM), transmission electron microscopy (TEM), and X-ray diffraction (XRD) measurements. MEAs with Ru(44.0 wt.%)Se(2.8 wt.%)/VulcanXC72 cathode catalyst achieved the highest performance of all $RuSe_x$ catalysts investigated, i.e. ~40 mW cm^{-2} at 80 °C under ambient pressure and $\lambda_{MeOH} = \lambda_{air} = 4$. This is 40% of the value obtained with commercial platinum cathode catalyst under the same operating conditions. The $RuSe_x$ catalysts investigated are stable over a period of more than 1,000 h. This was confirmed by TEM and XRD measurements, where no increase in mean $RuSe_x$ particle size (~5 nm) after fuel cell operation was found. Enhancement of specific catalyst activity, mass transport, and active surface offer potential for a further improvement of $RuSe_x$ catalyst layers.

Keywords Ru-Se · Methanol tolerant catalysts · DMFC cathodes · Surface roughness · XRD · CLSM · SEM · TEM

K. Wippermann (✉) · B. Richter · K. Klafki · J. Mergel
IEF-3, Forschungszentrum Jülich GmbH,
52425 Julich, Germany
e-mail: k.wippermann@fz-juelich.de

G. Zehl · I. Dorbandt · P. Bogdanoff · S. Fiechter
Hahn-Meitner-Institut-Berlin,
Glienicker Str. 100, 14109 Berlin, Germany

S. Kaytakoglu
Faculty of Engineering and Architecture, Anadolu University,
Eskisehir 26470, Turkey

1 Introduction

It is well known that the cathode of Direct Methanol Fuel Cell (DMFC) suffers mixed potential formation because of methanol cross over through the membrane. To overcome this problem either methanol impermeable membranes or methanol tolerant catalysts have to be developed, which selectively reduce oxygen. One of the more promising methanol tolerant catalysts are carbon supported ruthenium nano-particles with selenium-modified surfaces ($RuSe_x$). There are several studies on oxygen reduction on $RuSe_x$ [1–7, Zehl G et al., Fiechter S et al. Submitted]. However, only two of these present studies on the performance of $RuSe_x$ cathode catalyst layers as part of membrane electrode assemblies (MEAs) under DMFC operating conditions [6, 8] and none deal with the important issue of durability. In most cases, the performance of $RuSe_x$ catalysts is determined by rotating disc electrode (RDE) experiments with thin catalysts layers in aqueous sulfuric acid solution [2, 9].

There are several differences between fuel cell operation and RDE experiments: It is well-known that the adsorption of sulfate ions causes a significant loss of performance,

even though the utilization of catalyst is enhanced [10, 11]. Furthermore, the rate of oxygen transport through sulphuric acid + thin catalyst layer (RDE) or a gas diffusion electrode (MEA), and the oxygen concentration at the active sites may be different. The preparation procedure may also influence the performance. In RDE experiments, a thin catalyst layer of thickness less than 10 μm is usually prepared by dropping a dispersed catalyst suspension on a glassy carbon electrode and drying it in air at room temperature [9]. In contrast, the catalyst layers of MEAs usually have a thickness of more than 10 μm, if carbon supported catalysts are used and metal loading amounts to more than 0.5 mg cm^{-2}. These catalyst layers are usually hot-pressed onto either gas diffusion electrodes or decal foils at elevated temperatures and pressures, e.g. 130 °C and 0.5 kN cm^{-2} in the case of Nafion® (see Sect. 2).

Different operation and preparation conditions may also influence the relative performance of different catalysts. Therefore, the characterization of $RuSe_x$ catalysts under fuel cell operating conditions is essential to rate the quality of the catalysts in terms of performance. Moreover, long-term experiments over periods of 1,000 h and more are necessary to test durability.

The preparation and characterization of carbon supported ruthenium nano-particles surface modified with selenium ($RuSe_x$) have been described [8, Zehl G et al. Submitted]. The preparation and characterization of MEAs with cathode catalyst layers based on three selected carbon supported $RuSe_x$ catalysts are reported here. The aim of this work is to evaluate the best $RuSe_x$ catalyst regarding performance and durability under fuel cell operating conditions, and to improve MEA performance by modifying the structure and composition of $RuSe_x$ cathode catalyst layers. $RuSe_x$ cathode catalyst layers were characterized by modifying catalyst loading, PTFE and Nafion® content, and the fraction of $RuSe_x$ in the carbon supported catalysts. The MEAs and cathode catalyst layers were electrochemically characterized by recording polarization curves, galvanostatic measurements and impedance spectra. The morphology of the catalyst layers was investigated by confocal laser scan microscopy (CLSM), scanning electron microscopy (SEM), transmission electron microscopy (TEM), and X-ray diffraction (XRD) measurements. TEM and XRD were also used to determine the size of $RuSe_x$ particles before and after fuel cell operation.

2 Experimental

2.1 Preparation of membrane electrode assemblies (MEAs) and catalyst coated membranes (CCMs)

In most cases, the catalysts layers were prepared onto the gas diffusion layer ('GDL method') and then hot-pressed with a Nafion® 117 membrane (DuPont) at 130 °C and 0.5 kN cm^{-2} to obtain the complete MEA. In some cases, the catalyst layers were prepared on a suitable polymer substrate (so-called 'decal foil') and hot-pressed under the same conditions with the Nafion® 117 membrane. The decal foil was then removed, leaving the catalyst layers on the membrane and forming catalyst coated membranes ('CCM method'). By putting GDLs on both sides of the CCM, the complete MEA was obtained. Both methods yield the same MEA performance within limits of experimental error. MEAs made by the GDL method were used for performance and durability tests. In combined electrochemical and microscopic/spectroscopic investigations (see Figs. 9–12, 15), MEAs made by the CCM method were used.

Independent of the GDL or CCM method the catalyst layers were always prepared from catalyst inks using the roll-over knife technique. The catalyst inks contained isopropanol, catalyst particles, Nafion® (Ion Power) and, in some cases, PTFE (Charge 5032, Dyneon). Nafion® ionomer extends the reaction zone into the bulk of the catalyst layers, while PTFE acts as a hydrophobizing agent. The composition of all catalysts used and catalyst layers prepared are listed in Table 1. Two platinum reference

Table 1 Composition of catalysts and catalyst layers

Electrode	Catalyst	Catalyst layer		
		$RuSe_x$ or Pt loading (mg cm^{-2})	Nafion® fraction (wt.%)	PTFE fraction (wt.%)
Cathode	Ru(18.7 wt.%)Se(0.9 wt.%)/Vulcan XC72	0.5, 1.1, 2.0	30	0, 6, 18
	Ru(44.0 wt.%)Se(2.8 wt.%)/Vulcan XC72	0.5, 1.1, 1.9	20, 30, 40, 60	–
	Ru(37.6 wt.%)Se(6.4 wt.%)/BP2000	1.0	25	–
	Pt(40 wt.%)/C	2.0	30	–
	Pt(60 wt%)/C (HiSPEC 9000, Johnson Matthey)	1.1	20 (28)	–
Anode	Pt-Ru(60 wt%)/C (HiSPEC 9000, Johnson Matthey)	2.1–2.6	20 (30)	–

catalysts and three $RuSe_x$ catalysts were used. The anode catalyst was always the same, i.e. Pt–Ru(60%)/C (HiSPEC 10000, Johnson Matthey). The Nafion® content was adjusted according to the composition of the carbon supported catalysts.

Depending on the GDL or CCM method, GDLs or decal foils were used as substrates for preparation of the catalysts layers. The GDLs consisted of a thin micro-layer composed of Vulcan XC 72 and PTFE prepared on a E-TEK carbon cloth ('A' Cloth). For more details, see e.g. [12]. In the case of the CCM method, either Kaptone or Glass Fiber enforced PTFE from Reichelt Chemietechnik GmbH&Co. were used as decal foils. After preparing the CCMs, carbon cloth without micro-layer was used as GDL on both sides. This is important, because otherwise parts of the micro-layer would remain on the catalyst layer after removal of GDL and surface analysis of catalyst layer would be difficult.

The desired geometries of the electrodes were realized by using either masks (CCM method) or by cutting the electrodes by stamping tools from Marbach® Stanzformtechnik (MEA method). Two MEA/CCM geometries, here denoted as Type I and Type II, were used. For MEA/CCM Type I, both anode and cathode had a geometrical area of 4.7 cm^2 (1.1 × 4.3 cm). A third stripe with the same geometry served as a hydrogen reference electrode. The composition of the reference electrode was the same as the cathode. MEA/CCM Type I is used for short-term characterization in half cell and single cell modes. The short-term characterization includes periodical recording of U/I measurements of cells and electrodes over a period of about 3 days. The electrodes of MEA/CCM Type II were square-shaped with an area of 17.6 cm^2. This type of MEA/CCM does not contain a reference electrode and was only used for the single cell aging experiments over a period of 1,000 h.

2.2 Electrochemical measurements

The two types of MEAs and CCMs were characterized in two different tests cells, where the geometries of the graphite flow fields ('BBP4', SGL Carbon) and the stainless steel endplates were fitted to the geometries of the electrodes of MEA/CCM Type I and II. For all flow fields, a grid design (1 × 1 × 1 mm) was used. All measurements were carried out at a temperature of 80 °C, under ambient pressure and in counter flow mode. The anode was always fed by 1 M methanol solution and the cathode was purged with air. The stoichiometric factor λ of methanol and air was always four. The electrochemical measurements were performed by means of a Zahner IM 6 electrochemical workstation. This includes U/I-measurements of cells and electrodes as well as impedance spectra (amplitude: 10 mV, U_{DC} = 0.3 V) to determine the ohmic resistance.

2.3 Microscopic investigations (CLSM, SEM, TEM)

CLSM measurements of catalyst layers were performed with a CLSM, TCS SP2 (Leica) using an Argon Laser with a wavelength of 488 nm. This system allows imaging of a series of planes with a stack of serial optical sections through the catalyst layers and computation of composite projection images and volume-rendered 3-D representations of the samples. Furthermore, topographic profiles were determined and roughness factors of the catalyst layers were calculated according to the equation

$$P_a = \frac{1}{l}\int_0^l |Z(x)|\mathrm{d}x \quad (1)$$

with P_a/μm as the roughness factor, i.e. the average deviation from the mean surface height ($\overline{Z}$/μm), where $Z(x) = Z_i - \overline{Z}$, l/μm is the distance of measurement and x/μm is the ordinate along the surface of catalyst layer. Both $RuSe_x$ and Pt catalyst layers prepared on GDL were investigated. Before examination the samples were pressed at room temperature at 0.5 kN cm^{-2}.

SEM images of cross sections of CCMs broken under liquid nitrogen were taken in a LEO 1530 at 2 keV. TEM images were taken using a Philips CM 12 equipped with a super twin lens with a slow scan CCD camera and an X-ray fluorescence analyzer (EDX). The acceleration voltage was 120 kV. The samples were prepared by dispersing a small amount of catalyst in ethanol using an ultrasonic bath. One drop of this dispersion was then deposited onto a carbon-coated grid and left to dry at room temperature. X-ray fluorescence analysis was used to quantify the composition of the samples. Absolute metal content was analyzed by neutron activation analysis (NAA).

2.4 XRD measurements

XRD patterns were recorded from catalyst layer powder using a SIEMENS Diffractometer D500 (Cu $K\alpha_1$ radiation, λ = 0.154056 nm) at a scanning rate of 0.02° s^{-1} for 2Θ in the range 20–60°. The catalyst powders were scratched from the membrane of CCMs after 3 days operation.

3 Results and discussion

3.1 Characterization of MEAs with Ru(18.7 wt.%)Se(0.9 wt.%)/XC72 cathode catalyst

The first membrane electrode assemblies were prepared and characterized using a $RuSe_x$ cathode catalyst with the composition Ru(18%)Se(2.5%)/Vulcan XC72. Firstly, the

methanol tolerance of the prepared $RuSe_x$ cathode as part of a MEA was checked at open circuit conditions by passing the cathode exhaust gas through a saturated barium hydroxide solution for 2 h. During the whole experiment, the anode was supplied by 1 M methanol solution (0.1 mL min^{-1}) and the cathode purged with air (17 mL min^{-1}). For comparison, the same experiment was also carried out with a platinum cathode. According to Eq. 2, insoluble barium carbonate should be formed if the cathode is not methanol tolerant.

$$Ba(OH)_2 + CO_2 \rightarrow BaCO_3 \downarrow + H_2O \quad (2)$$

Traces of carbon dioxide included in the air flow of the cathode inlet also cause some precipitation of barium carbonate. This amount was determined in a blind test by passing the air directly through the barium hydroxide solution for two hours. After these experiments, the precipitated barium carbonate was filtered, oven dried at 60 °C and weighed. The values obtained with $RuSe_x$ and Pt cathodes were corrected by subtracting the blind value. In the case of the MEA with platinum cathode catalyst, the permeating methanol reacts with oxygen by forming 280 mg carbon dioxide, resulting in precipitation of 1,250 mg $BaCO_3$. This correlates with a "reasonable" methanol permeation current density at open circuit conditions of 93 mA cm^{-2}. For the MEA with $RuSe_x$ cathode catalyst, no precipitation was obtained after subtracting the blind value. This means that $RuSe_x$ is indeed a selective catalyst for oxygen reduction and is highly methanol tolerant under DMFC operating conditions. This is in agreement with RDE measurements in sulfuric acid, which indicate no change in the current characteristics in the presence of methanol [8].

The performance of MEAs with $RuSe_x$(20%)/XC72 and Pt(40%)/C cathode catalysts is shown in Fig. 1. There are two important features of this diagram:

(a) The maximum power density obtained with $RuSe_x$ cathode catalyst compared to platinum is a factor of 2.4 smaller (28 vs. 66 mW cm^{-2}) and the power density at a cell voltage of 400 mV is 3.3 times smaller (17 vs. 56 mW cm^{-2}). The lower activity of $RuSe_x$ towards oxygen reduction in comparison with Pt is well-known from RDE measurements [1–3, 6, 8Zehl G et al.]. However, Neergat et al. [5] reported a higher specific activity of large carbon supported $RuSe_x$ particles (d = 20 nm) compared to small Pt/C particles (d = 3 nm), despite the higher mass activity of platinum. However, the $RuSe_x$(20%)/XC72 catalyst has an intrinsic disadvantage compared to the platinum catalysts: The amount of $RuSe_x$ in the catalyst (20%) is only one half and one third, respectively, of the amount of platinum in the reference catalysts. Moreover, Ru and Se have densities of 12.1 and 4.8 mg cm^{-3} (T = 20°C, [13]), much smaller than that of Pt

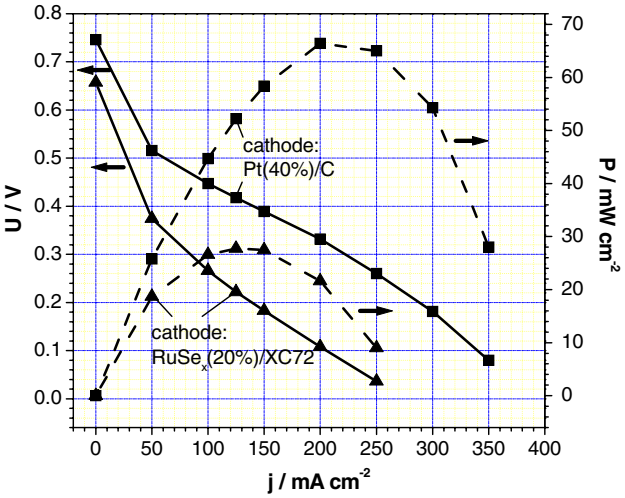

Fig. 1 U/j and P/j characteristics of MEAs with Ru(18.7 wt.%)-Se(0.9 wt.%)/XC72 (▲, 2.0 mg$RuSe_x$ cm^{-2}) and Pt(40%)/C (■, 2.0 mg Pt cm^{-2}) cathode catalysts, T = 80 °C, ambient pressure, $\lambda_{air} = \lambda_{MeOH} = 4$

(21.5 mg cm^{-3} [13]). Assuming the same loading, this results in significantly thicker catalyst layers for the $RuSe_x$ catalyst: By means of a caliper, values of 110 ± 5 µm for the $RuSe_x$ catalyst layer and 35 ± 5 µm for the Pt catalyst layer were determined. Possible disadvantages are a higher overpotential of oxygen diffusion and a lower amount of $RuSe_x$(20%)/XC72 in the active zone of the catalyst layer near the membrane, corresponding to a dissolution effect of $RuSe_x$ catalyst particles: If one assumes an exponential decay of the electrochemical current from the surface of the membrane into the bulk of the catalyst layer, the so-called 'penetration depth' indicates the distance from the membrane surface, where the electrochemical current decreases to a fraction of 1/e the value at the membrane surface [14]. The first sub-layer within the penetration depth is highly electro-active, whereas the second sub-layer, which is adjacent to the backing layer has a low electrochemical activity [14]. The penetration depth depends on the specific proton conductivity, σ_{H^+}/S cm^{-1}, and the electrochemical volume resistivity, R_i/Ω cm^3, as follows [14]:

$$\lambda = \sqrt{(\sigma_{H^+} * R_i)} \quad (3)$$

If one assumes the proton conductivity of $RuSe_x$/C catalyst layers to be comparable to that of Pt/C, the difference in penetration depth would predominantly be caused by the change in electrochemical volume resistivity. Because of the smaller catalytic activity, the electrochemical volume resistivity of $RuSe_x$/C catalyst layers is about 2-fold higher compared to Pt/C layers. Hence, the penetration depth in the $RuSe_x$ layers should be roughly a

factor 1½ higher than similar Pt/C layers (e.g. same fraction of metal in catalyst, same volume fraction of Nafion® in catalyst layer and same Nafion® distribution) under the same operating conditions. If the catalyst layer is much thicker than the penetration depth, only a part of the catalyst particles will be highly active. Even fewer particles will be active because only a certain part of the catalyst particles laying within the penetration depth is contacted by Nafion® and is electro-active. As can be deduced from Eq. 3, the penetration depth increases with Nafion® content of the catalyst layer. This has been already validated for platinum catalyst layers [14, 15], insofar as the penetration depth can be adapted to the particular thickness of catalyst layer. This adaption is limited, however, because higher fractions of Nafion® lead to a decrease in active surface due to unfavorable Nafion® distribution [14, 15] and to mass transport limitations caused by blocking of the Nafion® phase [14, 15]. For example, it was found that the best performance of a Pt(60%)/C catalyst layer is obtained with a Nafion® fraction of 20 wt.%, corresponding to a penetration depth of only 40% of the layer thickness [15].

(b) The open cell voltage of the MEA with $RuSe_x$ cathode is about 100 mV lower than that of platinum. This result is astonishing, since methanol oxidation is not taking place on the $RuSe_x$ cathode and thus no mixed potential can be established. Even if the usual fluctuation of the OCV with an uncertainty of about ±50 mV is taken into account, one would have expected a pronounced increase in cathode potential with respect to the OCV in the presence of $RuSe_x$.

The half cell measurements in Fig. 2 reveal that the low OCV is mainly caused by the low cathode potential of about 700 mV. This is in contrast with cathode potentials of more than 900 mV achieved with $RuSe_x$ electrodes in 1 M sulfuric acid, even in the presence of 1 M methanol [Zehl G et al. Submitted]. The potential of the $RuSe_x$ cathode under load is, on average, 200 mV lower than that of the Pt cathode. This means, that the superior performance of the Pt-MEA is solely due to the higher activity of the Pt catalyst layer. The potentials of the "identical" Pt/Ru anodes deviate by about 30 mV, which lies within the range of experimental error.

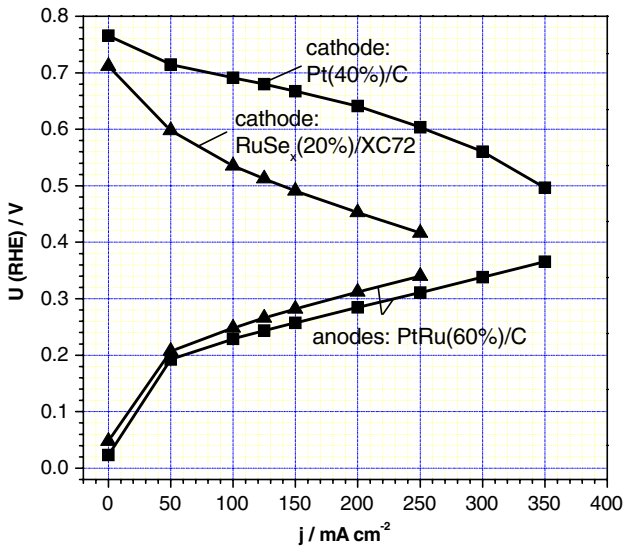

Fig. 2 U/j characteristics of cathodes with Ru(18.7 wt.%)-Se(0.9 wt.%)/XC72 (▲, 2.0 mg $RuSe_x$ cm^{-2}) and Pt(40%)/C (■, 2.0 mg Pt cm^{-2}) catalysts and anodes with PtRu(60%)/C catalyst, T = 80 °C, ambient pressure, $\lambda_{air} = \lambda_{MeOH} = 4$

Possible explanations for the low open circuit voltage of MEAs with $RuSe_x$ cathodes are (i) a reduction of oxygen concentration and (ii) a change of reaction mechanism:

(i) The thicker the catalyst layer, the slower the oxygen transport and the lower the oxygen concentration in the inner, active part of the catalyst layer. However, the effect is small: Per decade of oxygen partial pressure difference, the potential changes by only 17 mV according to the Nernst equation. To lower the OCV from 900 to 700 mV versus RHE, the oxygen partial pressure must decrease by more than ten orders of magnitude, which is improbable. The small effect of oxygen partial pressure was validated by running the cathode with mixtures of nitrogen and oxygen in a partial pressure range 5×10^3–5×10^4 Pa. The OCV increased by 18 mV from 657 to 674 mV/RHE, which is close to the Nernst prediction. Another reason for decreased oxygen concentration may be enhanced flooding of $RuSe_x$ catalyst layers because of the more hydrophilic nature of $RuSe_x$ compared to Pt. This is supported by lower contact angles of water droplets (sessile drop method) on $RuSe_x$ catalyst layers (121–129°) compared to a Pt catalyst layer (139°) (Zehl G Unpublished results). It should be noted that the contact angle is strongly dependent on the nature of the carbon support and the roughness/porosity of the surface [16]. Therefore, the values of contact angles may only serve as a first, qualitative indication of the hydrophilic behavior of $RuSe_x$.

(ii) It has been reported, that the reduction of oxygen on $RuSe_x$ proceeds not only in a four electron reduction mechanism, but also via hydrogen peroxide as a side reaction [2, 3, 7, Zehl G et al. Submitted]. The equilibrium potential of the two electron reduction from oxygen to peroxide amounts to 0.695 V/RHE [17]. The kinetics of the four electron and the two electron mechanisms depend to some extent on the proton and oxygen concentrations. A change in these concentrations will lead to a changed ratio of the two mechanisms and therefore to a shift of the mixed potential. Whereas the proton conductivity within the electrolyte (RDE measurements) is assumed to be high, it is possible that the conductivity of the thin Nafion® layer may limit the proton diffusion kinetics. A lower proton concentration would favor the two electron mechanism resulting in a smaller open circuit potential. However, the

amount of generated peroxide is reported to be only a few percent [2, 3, 7, Zehl G et al. Submitted]. In conclusion, there is no satisfactory theory at the moment, which is able to explain the unexpected low OCV as well as the difference between MEA operation and the model system.

To improve the performance of the $RuSe_x$ cathode catalyst layers several modifications were carried out and they are summarized in Table 2. The $RuSe_x$ loading was reduced from 2 to 1 and 0.5 mg cm^{-2}. The performance of the corresponding MEAs is shown in Fig. 3. If $RuSe_x$ loading is reduced from 2 to 1 mg cm^{-2}, the maximum power density increases by 4 mW cm^{-2}. This means that the positive effect of improved oxygen transport caused by lower catalyst layer thickness dominates. By means of a caliper, a decrease in layer thickness from 110 ± 5 µm (2 mg $RuSe_x$ cm^{-2}) to 65 ± 5 µm (1 mg $RuSe_x$ cm^{-2}) was measured. A further reduction of $RuSe_x$ loading to 0.5 mg cm^{-2} leads to a decrease in maximum power density by 10 mW cm^{-2}. In this case the negative effect of a lower active surface prevails, despite a further reduction of catalyst layer thickness to 30 ± 5 µm. Unfortunately, there is no suitable method available to determine the active surface of $RuSe_x$ catalysts in MEAs. Because $RuSe_x$ does not adsorb methanol or CO, methods like methanol/CO stripping or CO-adsorption in the gas phase [18, 19] cannot be applied.

The second modification carried out was the addition of PTFE as hydrophobizing agent. As shown in Fig. 4, the addition of 6 and 18 wt.% PTFE to the catalyst layer caused a pronounced decrease in maximum power density by more than 10 mW cm^{-2}. It is evident, that the favorable hydrophobizing effect is overcompensated by detrimental effects like those listed in Table 2, e.g. increase in thickness of the catalyst layer. Indeed, the catalyst layer thickness increases from 65 ± 5 µm (without PTFE) to 95 ± 5 µm (18 wt.% PTFE). Based on these results, we abandoned adding PTFE and subsequently prepared the

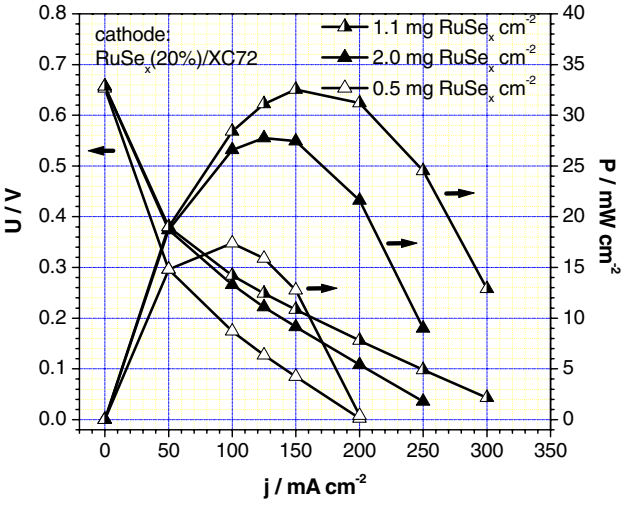

Fig. 3 U/j and P/j characteristics of MEAs with different $RuSe_x$ loadings (0.5/1.1/2.0 mg cm^{-2}) in Ru(18.7 wt.%)Se(0.9 wt.%)/XC72 cathode catalyst layers, T = 80 °C, ambient pressure, $\lambda_{air} = \lambda_{MeOH} = 4$

Table 2 Modifications of $RuSe_x$ catalyst layers

Modification	Possible consequences	Effect
1. Reduction of $RuSe_x$ loading at the same composition, → decrease of catalyst layer thickness	– Improved oxygen transport	⊕
	– Less waste of catalyst, thickness of catalyst layer closer to penetration depth	⊕
	– Lower active surface	⊖
2. Hydrophobization of catalyst layer, e.g. by addition of PTFE	– Less flooding, improved oxygen transport	⊕
	– Thicker catalyst layer, if constant catalyst loading	⊖
	– Less catalyst particles contacted by Nafion®, lower active surface	⊖
	– Problem of water transport	⊖
3. Higher amount of $RuSe_x$ in carbon supported catalyst → decrease of catalyst layer thickness at the same $RuSe_x$ loading	– Improved oxygen transport	⊕
	– More catalyst particles within the active zone of catalyst layer ('penetration depth')	⊕
	– Higher particle size, lower active surface	⊖
4. Enhancement of specific catalytic activity of $RuSe_x$ towards O_2 reduction, e.g. by changing the surface composition of the $RuSe_x$ particles and/or changing particle size	– Faster reduction of oxygen	⊕
5. Carbon support with higher specific surface, decrease of $RuSe_x$ particle size	– Higher active surface	⊕
	– Lower utilization because of inactive $RuSe_x$ particles in small pores	⊖

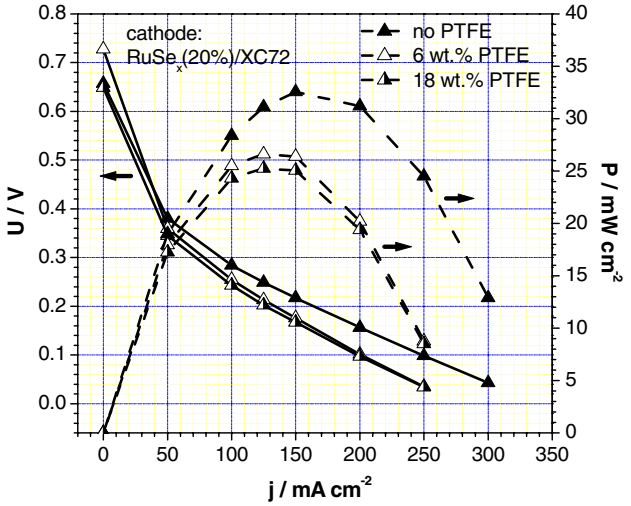

Fig. 4 U/j and P/j characteristics of MEAs with different PTFE contents (0/6/18 %) in Ru(18.7 wt.%)Se(0.9 wt.%)/XC72 cathode catalyst layers, 1.0 mg RuSe$_x$ cm^{-2}, T = 80 °C, ambient pressure, $\lambda_{air} = \lambda_{MeOH} = 4$

RuSe$_x$ cathode catalyst layers with a RuSe$_x$ loading of 1 mg cm^{-2} instead of 2 mg cm^{-2}.

Finally, a modification of the catalyst preparation, composition, and carbon support was carried out, corresponding to modifications No.3–5 in Table 2.

3.2 Characterization of MEAs with modified RuSe$_x$ cathode catalysts

Initially, the amount of RuSe$_x$ in the supported catalyst was enhanced from 20 to 47 wt.%. At the same time, the atomic ratio of Ru and Se decreased from Ru:Se = 16:1 for Ru(18.7 wt.%)Se(0.9 wt.%)/XC72 to Ru:Se = 12:1 for Ru(44.0 wt.%)Se(2.8 wt.%)/XC72. The second modification of RuSe$_x$ catalyst was a substitution of Vulcan XC 72 by Black Pearls BP2000 carbon support. The specific surface of BP2000 amounts to 1,445 m^2 g^{-1}, 6-fold higher than the value of Vulcan XC 72 (245 mg cm^{-2}). In this case, the atomic ratio of Ru and Se decreased significantly from Ru:Se = 16:1 for Ru(18.7 wt.%)Se(0.9 wt.%)/XC72 to Ru:Se = 5:1 for Ru(37.6 wt.%)Se(6.4 wt.%)/BP2000. Previous RDE investigation reveals a significantly higher catalytic activity of the Black Pearl based preparations towards oxygen reduction in sulfuric acid. This is assumed to be due to an optimized ruthenium to selenium ratio [Zehl G et al. Submitted].

The performance of MEAs prepared with different RuSe$_x$ cathode catalysts in comparison with a platinum reference MEA is summarized in Figs. 5 and 6. The RuSe$_x$ and Pt loadings in the cathode catalyst layers were about 1 mg cm^{-2}. The increase in amount of RuSe$_x$ from 20 wt.% (▲) to 47 wt.% (●) causes an improvement in cell performance

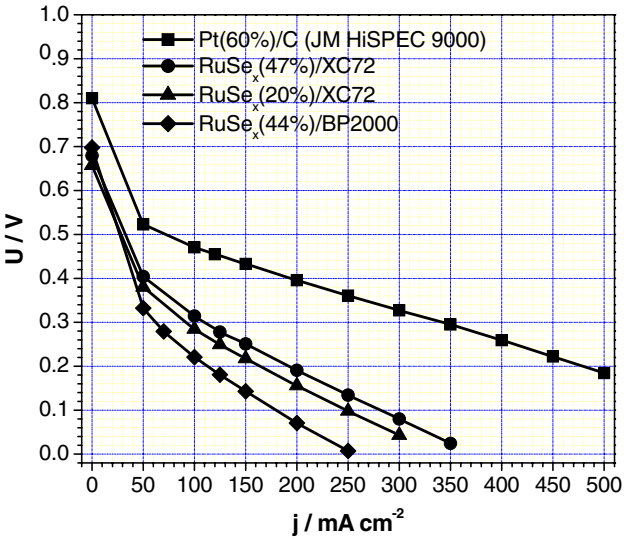

Fig. 5 U/j characteristics of MEAs with Pt(60%)/C (■, 1.3 mg Pt cm^{-2}) and three different RuSe$_x$ cathode catalysts: Ru(44.0 wt.%)Se(2.8 wt.%)/XC72 (●, 1.1 mg RuSe$_x$ cm^{-2}) Ru(18.7 wt.%)Se(0.9 wt.%)/XC72 (▲, 1.1 mg RuSe$_x$ cm^{-2}) and Ru(37.6 wt.%)Se(6.4 wt.%)/BP2000 (◆, 1.0 mg RuSe$_x$ cm^{-2}), T = 80 °C, ambient pressure, $\lambda_{air} = \lambda_{MeOH} = 4$

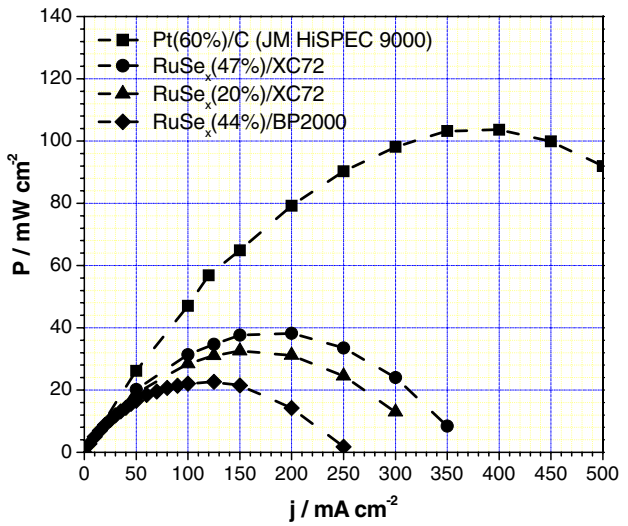

Fig. 6 P/j characteristics of MEAs shown in Fig. 5

from P_{max} = 32 mW cm^{-2}/$P_{0.4\ V}$ = 18 mW cm^{-2} to P_{max} = 38 mW cm^{-2}/$P_{0.4\ V}$ = 21 mW cm^{-2}. The increase in power density can be partly explained by faster mass transport due to decreased thickness of the cathode catalyst layer from 65 ± 5 μm (20 wt.% RuSe$_x$/C) to 25 ± 5 μm (47 wt.% RuSe$_x$/C). TEM images reveal (Fig. 7) that the 47 wt.% RuSe$_x$/C contains larger particles (5.1 nm) than the 20 wt.% RuSe$_x$/C catalyst. Thus, the electrochemically active surface of the 47 wt.% RuSe$_x$/C catalyst is not twice that of the 20 wt.% RuSe$_x$/C catalyst. Consequently, doubling the

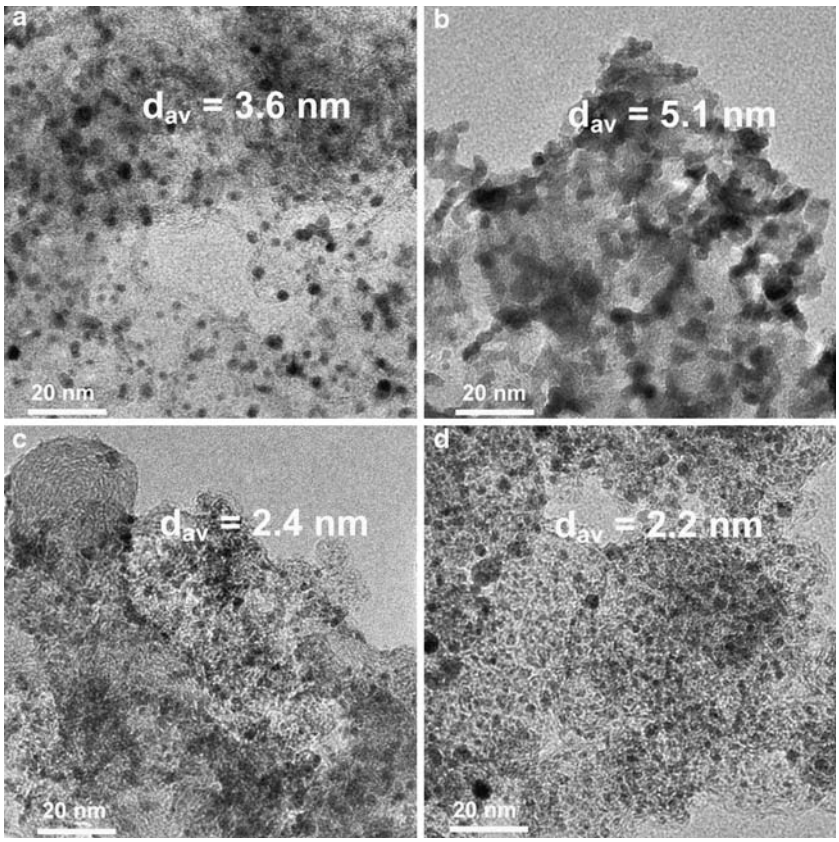

Fig. 7 Transmission electron micrographs of different catalyst powders: (**a**) Pt(40%)/C, (**b**) Ru(44.0 wt.%)Se(2.8 wt.%)/XC72, (**c**) Ru(18.7 wt.%)Se(0.9 wt.%)/XC72, (**d**) Ru(37.6 wt.%)Se(6.4 wt.%)/BP2000

ruthenium content will not result in doubling of current density. Furthermore, as discussed in [Zehl G et al. Submitted], the specific activity is strongly influenced by the surface composition of the $RuSe_x$ particles. Taking into account the selenium content and the different surface area of both catalysts, a different composition of the ruthenium surface has to be assumed. At this point we cannot yet precisely estimate the influence of these superposed factors on the specific activity. Nevertheless, in RDE analysis higher catalytic activity was obtained on the 47 wt.% $RuSe_x$/C catalyst compared to the 20 wt.% $RuSe_x$/C catalyst, which is in agreement with the DMFC measurements.

The second modification, i.e. substitution of carbon support Vulcan XC 72 by BP2000 yielded the worst MEA performance. As shown in Figs. 5 and 6, power densities of only P_{max} = 23 mW cm^{-2} and $P_{0.4V}$ = 15 mW cm^{-2} were achieved. This is unexpected because in RDE measurements this kind of catalyst leads to the highest current densities in oxygen reduction due to an optimized ruthenium to selenium ratio [Zehl G et al. Submitted]. Therefore, the specific catalytic activity seems to not be responsible for the bad DMFC performance. A possible explanation is the lower catalyst utilization because of more or less inactive $RuSe_x$ particles located in the small pores of the BP2000 carbon support. This agrees with results of Rao et al. [19], who found a pronounced decrease in the utilization of carbon supported Pt–Ru catalyst with increased specific carbon surface. They explained their results on the basis of the incompatibility between the morphological structure of the carbon support and Nafion® micelles: Carbon supports with high specific surface like BP2000 have a high amount of pores with a diameter of d < 20 nm. The large Nafion® micelles (d > 40 nm) [20, 21] do not penetrate into the smaller pores. Thus, a substantial amount of the catalyst particles is not electroactive.

The size of the catalytically active particles is another important parameter, which influences the active surface. Figure 7 shows transmission electron micrographs of the three $RuSe_x$ catalysts and the Pt(40%)/C reference catalyst for comparison. By means of the image processing and analysis program 'ImageJ', the mean diameter of $RuSe_x$ and Pt particles was determined from the TEM pictures. The Pt(40%)/C reference catalyst has a mean particle size d_{av} of 3.6 nm. Assuming spherical geometry of Pt and $RuSe_x$ particles, theoretical roughness factors may be estimated, i.e. dimensionless ratios of the entire surface of Pt or $RuSe_x$ per geometrical surface. For a catalyst layer prepared by 1 mg cm^{-2} of the Pt(40%)/C reference catalyst, a theoretical roughness factor of 780 was calculated. As expected, the $RuSe_x$ catalyst with the largest fraction of

$RuSe_x$ (47 wt.%) and a carbon support with a moderate BET surface (Vulcan XC72) has the largest $RuSe_x$ particles with a mean diameter DA of 5.1 nm, corresponding to the lowest platinum surface (see Fig. 7b). For a loading of 1 mg cm^{-2}, a roughness factor of the Ru(44.0 wt.%)-Se(2.8 wt.%)/XC72 catalyst layer of 980 was estimated. The second-best $RuSe_x$ catalyst with composition Ru(18.7 wt.%)Se(0.9 wt.%)/XC72, has smaller particles with only a mean particle size of 2.4 nm, corresponding to a roughness factor of 1,380 (see Fig. 7c). This may be due to the higher distance of the $RuSe_x$ particles on the carbon surface, which hinders the particle agglomeration. On the top left of Fig. 7c, a carbon particle with typical diameter of about 30 nm can be seen. The Ru(37.6 wt.%)-Se(6.4 wt.%) catalyst supported on BP2000 has the smallest mean $RuSe_x$ particle size of 2.2 nm (see Fig. 7d). This corresponds to a theoretical roughness factor of 1,470. It is striking, that the high surface of the Ru(18.7 wt.%)-Se(0.9 wt.%)/XC72 and Ru(37.6 wt.%)Se(6.4 wt.%)/BP2000 catalysts do not lead to a high MEA performance. Obviously, the advantage of a high particle surface is counteracted by the factors discussed above, i.e. lower utilization, smaller specific catalyst activity or poor mass transport.

In conclusion, the Ru(44.0 wt.%)Se(2.8 wt.%)/XC72 cathode catalyst yielded the best performance of the $RuSe_x$ catalysts investigated and we therefore focused our work on this catalyst. However, the P_{max} and $P_{400\ mV}$ values of the MEA prepared with this catalyst still amount to only 37% and 28%, respectively of the values obtained with the platinum reference MEA (see Fig. 6).

3.3 Characterization of MEAs with Ru(44.0 wt.%)Se(2.8 wt.%)/XC72 cathode catalyst

The superior performance of the MEA with Ru(44.0 wt.%)Se(2.8 wt.%)/XC72 cathode catalyst compared to Ru(18.7 wt.%)Se(0.9 wt.%)/XC72 catalyst can be partly explained by a decrease in layer thickness and faster mass transport. Because catalyst layers based on Ru(44.0 wt.%)Se(2.8 wt.%)/XC72 are about a factor of 2–3 times thinner than Ru(18.7 wt.%)Se(0.9 wt.%)/XC72 at the same $RuSe_x$ loading, mass transport problems should play a smaller role. If this is so, an increase in Ru(44.0 wt.%)Se(2.8 wt.%)/XC72 loading to more than 1 mg cm^{-2} should not be as detrimental as in the case of Ru(18.7 wt.%)Se(0.9 wt.%)/XC72. This is demonstrated in Fig. 8, where the performance of MEAs with different Ru(44.0 wt.%)Se(2.8 wt.%)/XC72 loadings are shown. An increase in $RuSe_x$ loading from 1 to 2 mg cm^{-2} yields the same performance, but no deterioration as in the case of Ru(18.7 wt.%)Se(0.9 wt.%)/XC72 (compare Fig. 3). Here, the negative effect of slower oxygen transport is exactly compensated for by the positive effect of higher $RuSe_x$ surface available for oxygen reduction. This suggests that a further increase in $RuSe_x$ fraction in the carbon supported catalyst may induce an even better performance at $RuSe_x$ loadings higher than 1 mg cm^{-2}.

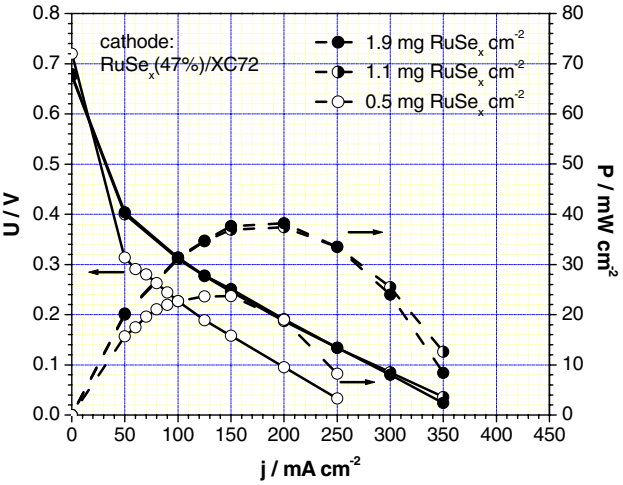

Fig. 8 U/j and P/j characteristics of MEAs with different $RuSe_x$ loadings (0.5/1.1/1.9 mg cm^{-2}) in Ru(44.0 wt.%)Se(2.8 wt.%)/XC72 cathode catalyst layers, T = 80 °C, ambient pressure, $\lambda_{air} = \lambda_{MeOH} = 4$

Microscopic investigations of the morphology of Ru(44.0 wt.%)Se(2.8 wt.%)/XC72 cathode catalyst layers as part of CCMs were also carried out. The surfaces of the catalyst layers were examined by confocal laser scanning microscopy (CLSM, see Sect. 2). Figure 9a/b shows top views of the surface of the Pt(40%)/C reference catalyst layer (Fig. 9a) and Ru(44.0 wt.%)-Se(2.8 wt.%)/XC72 catalyst layer (Fig. 9b). The area scanned by the laser beam was 1.5 by 1.5 mm. For the labeled areas on the images of the catalyst layers the surface roughness was determined. The surface roughness values, P_a, which are indicated on the images, were calculated using Eq. 1. On average, the same P_a values of 2.5 ± 0.5 µm were obtained for both catalyst layers, indicating a similar surface roughness. However, on a larger scale, the platinum catalyst layer appears to be rougher than the $RuSe_x$ layer, as can be seen more clearly from Fig. 10a/b, where three-dimensional plots of the surface topography of both catalyst layers are shown. Moreover, the microstructures of the layers are different: The platinum catalyst layer shows a structure with many fine cracks (width ≤ 20 µm) and a few rough cracks (width > 20 µm). In contrast, the $RuSe_x$ catalyst layer shows preferentially rough cracks. Image analysis of Fig. 9a/b yielded a more open structure for the platinum catalyst layer (Fig. 9a) with an overall area fraction of the cracks of 8 ± 1%. The $RuSe_x$ catalyst layer (Fig. 9b) shows a crack fraction of only 4 ± 1%. Additionally, a

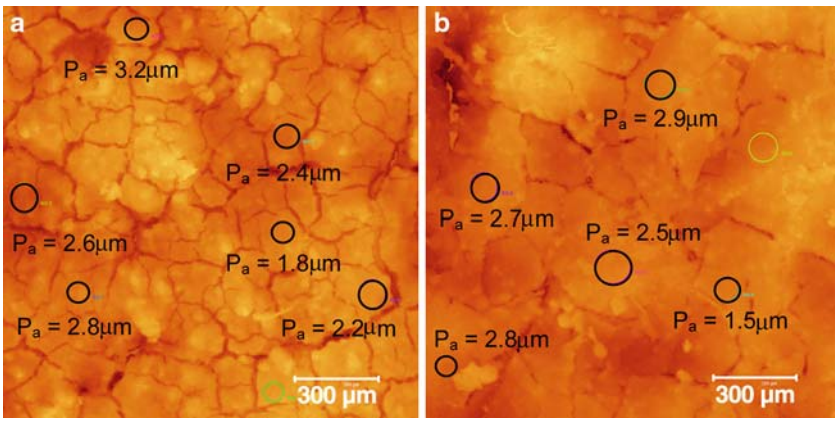

Fig. 9 Confocal Laser Scan Miscroscope (CLSM) pictures of cathode catalyst layers as part of CCMs: (**a**) Pt(60%)/C, (**b**) Ru(44.0 wt.%)Se(2.8 wt.%)/XC72; scan area: 1.5 × 1.5 mm; top view; roughness values, P_a, were calculated for the circular areas indicated

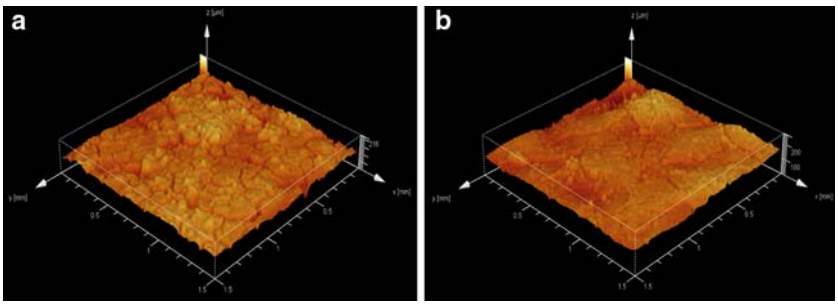

Fig. 10 CLSM pictures of Fig. 9, 3-D representation

topography profile analysis was carried out for both catalyst layers and results are shown in Fig. 11a/b. The profiles were determined along the dotted lines on the surface of the catalyst layers indicated in the same figure. The fine cracks in the platinum catalyst layer (see Fig. 11a) have a depth of 20 µm, which fits fairly well to the layer thickness. The rough cracks in both catalyst layers with a depth of 40–60 µm are extending into the underlying GDL (see Fig. 11a/b). They originate from cracks formed in the micro layer of the GDL during the drying process prior to preparation of the catalyst layer. The more open structure of the platinum catalyst layer with fine and rough cracks may be advantageous for mass transport, especially oxygen diffusion. From this point of view, the morphology and microporosity of the $RuSe_x$ catalyst layer may provide some potential for improvement of structure and performance.

The microstructure across the catalyst layer employing Ru(44.0 wt.%)Se(2.8 wt.%)/XC72 was investigated by SEM. This catalyst layer was part of a CCM and the sample was broken under liquid nitrogen. Figure 12a shows a SEM picture of the interface of the $RuSe_x$ layer and the Nafion® membrane. The microstructure is similar to that of platinum catalyst layers, i.e. a highly porous structure formed by supported catalyst particles (d ca. 30 nm) and Nafion® micelles (d > 40 nm). The right of Fig. 12a and b show a film-like structure of Nafion®, which covers an area of some µm^2. Obviously, the distribution of Nafion® within the $RuSe_x$ catalyst layer is not uniform. This implies accumulation of Nafion® in one part of the catalyst layer and at the same time, depletion of Nafion® in other parts. Accumulation may cause blocking of oxygen transport, and depletion may induce decreased catalyst utilization due to lack of contact between catalyst and

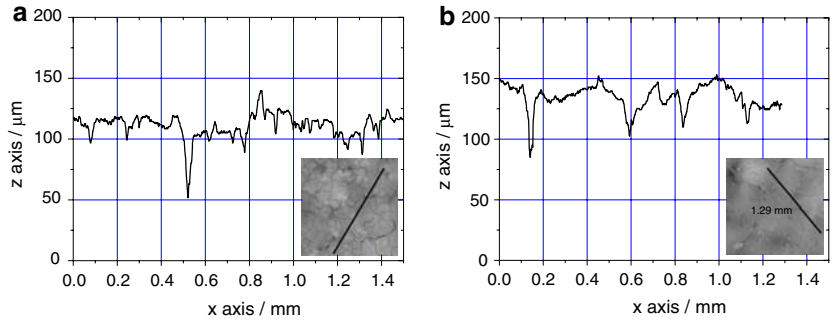

Fig. 11 Roughness profiles of the samples shown in Figs. 9/10; profiles determined along the lines indicated on the CLSM pictures included in the figure

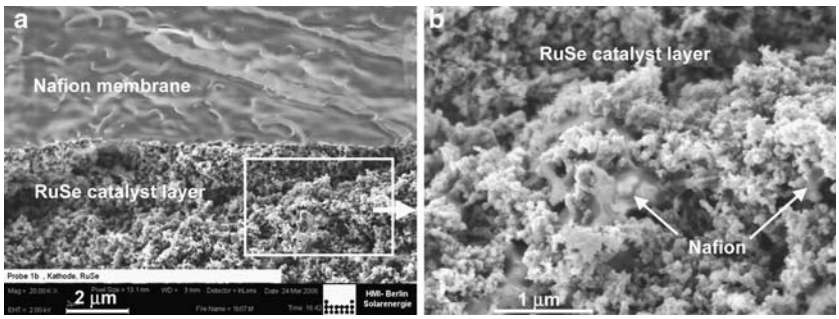

Fig. 12 Scanning electron micrographs of the cross section of a Ru(44.0 wt.%) Se(2.8 wt.%)/XC72 catalyst layer prepared on a Nafion® 117 membrane (part of CCM); (**a**) interface Nafion membrane/ $RuSe_x$ catalyst layer (**b**) three-fold magnification of the detail denoted in (**a**)

Nafion® particles. Therefore, it is not only important to achieve a suitable volume fraction of Nafion® within the catalyst layer, but also to achieve homogeneous distribution of the ionomer.

3.4 Durability tests of MEAs with Ru(44.0 wt.%)Se(2.8 wt.%)/XC72 cathode catalyst

The durability of $RuSe_x$(47%)/XC72 catalyst was checked under galvanostatic DMFC operating conditions over a period of 1,000 h using MEA type II (Electrode area ~18 cm^2, see Sect. 2). As seen from Fig. 13, the experiment was started with a current density of 142 mA cm^{-2} (2.5A). After 200 h the cell voltage dropped below 100 mV and the current density was reduced to 114 mA cm^{-2} (2A). During the last 180 h, the current density was again increased to 142 mA cm^{-2}. From time to time, the measurement was interrupted to determine characteristics like power density, ohmic resistance, and water permeation. After each interruption, the cell voltage started at a higher value than before interruption and then decreased exponentially. This behavior is not particularly due to the $RuSe_x$ catalyst, but typical for DMFC MEAs and can be attributed to reversible aging effects like cathode flooding [22].

The characteristic values determined during interruptions of the galvanostatic experiment are plotted in Fig. 14 versus operation time. The maximum power density (●) and the power density at a cell voltage of 400 mV (○) show similar time dependence. The maximum power density starts at 20 mW cm^{-2} and decreases over the first 360 h by about 20%, but then remains almost constant at about 17 mW cm^{-2}. This result is surprising, since MEAs of both types do not usually show any difference in performance, if platinum is the cathode catalyst. A possible reason discussed above may be enhanced flooding of the more hydrophilic $RuSe_x$ layer, reducing the oxygen concentration especially near the oxygen outlet. Such effects should be more pronounced if electrode area is higher and the oxygen distribution is more inhomogeneous.

Apart from the first value of ohmic resistance obtained after 26 h, the time dependent change in ohmic resistance is opposed by the change in maximum power density. However, changes in ohmic resistance have no significant influence on the power density. Because the maximum power densities are reached at current densities of

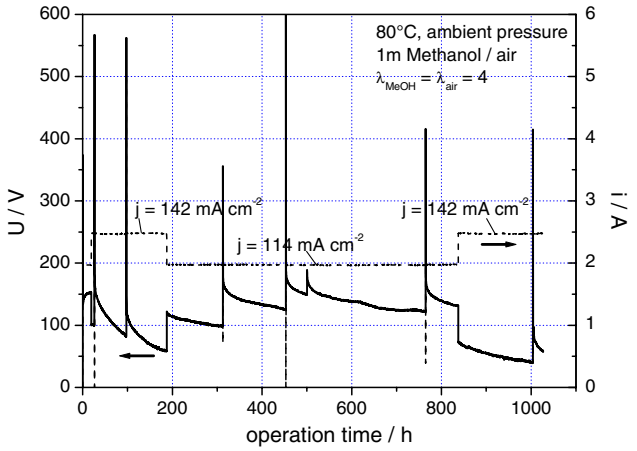

Fig. 13 Galvanostatic aging test of a MEA with Ru(44.0 wt.%)-Se(2.8 wt.%)/XC72 cathode catalyst layer; $RuSe_x$ loading: 1.1 mg cm^{-2}; current density 114 and 142 mA cm^{-2}, as indicated

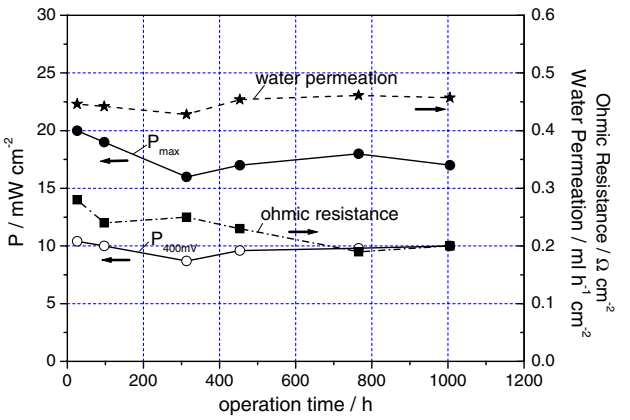

Fig. 14 Change of power densities (P_{max}, $P_{400\ mV}$), water permeation rate and ohmic resistance during the galvanostatic aging test shown in Fig. 13

70–100 mA cm^{-2}, the change in specific ohmic resistance up to 0.08 Ω cm^2 causes a difference in power density of only 0.6–0.8 mW cm^{-2}, which is less than 20% of the change of P_{max} (4 mW cm^{-2}) as indicated in Fig. 14. This means, that the change in power density during the first 400 h is due to deteriorated mass transport. Because the rate of water permeation (★) of about 0.45 mL h^{-1} cm^{-2} stays more or less constant (see Fig. 14), flooding of the cathode catalyst layer or GDL may be caused by more thorough wetting of the micro-pores. The wetting process may be supported by an increase in hydrophilicity of the inner electrode surface due to an oxidation of carbon surface groups or a loss of PTFE [23].

The almost constant performance of the $RuSe_x$ based MEA after 360 h of operation time until the end of the experiment means that $RuSe_x$ is a stable catalyst under the operating conditions indicated above. There are few experiments concerning durability of non-platinum catalysts, mostly macro cycle transition metal complexes [24, 25]. But even short-term experiments reveal pronounced aging of these non-platinum catalysts, especially by formation of hydrogen peroxide and peroxyl radicals, which degrade perfluorinated sulfonic acid membranes [26] or may even attack the catalyst itself [24]. We believe that the durability tests presented here are the first experiments on non-platinum catalysts over a period of more than 1,000 h.

A well-known aging effect of platinum catalysts is the coarsening of platinum particles associated with a decrease in active surface and performance. In PEM Fuel Cells, the coarsening effect is significantly enhanced by voltage cycling [27]. Ferreira et al. [27] investigated the platinum coarsening mechanism and identified 3D-Ostwald ripening and migration of soluble platinum cations from the cathode toward the membrane as the two aging processes responsible for the platinum area loss.

A possible coarsening of $RuSe_x$ and Pt particles in cathode catalyst layers made by $RuSe_x$(47%)/XC72 and Pt(40%)/C reference catalyst was investigated. XRD analysis (Fig. 15) was performed on the pristine $RuSe_x$ catalyst CCM, as well as on the used one after short-term measurements with CCM Type I in DMFC (~5 days, see Sect. 2). Additionally, in Fig. 15, XRD measurement of the used platinum CCM is shown, which depicts the typical pattern of metallic cubic phase platinum. The spectra of the $RuSe_x$ catalysts reveal a broadened signal pattern of metallic ruthenium in accordance with previous investigations [2, 3], which points towards metallic Ru nanoparticles. Based on Scherrer analysis, the volume-weighted average grain size, DV, of $RuSe_x$ is calculated for the pristine and the used catalyst, using the Ru[101] reflex. Due to the broadening of the signal a reliable evaluation of the particle sizes via the Scherrer equation alone is not appropriate. However, from the fact that the spectra of the

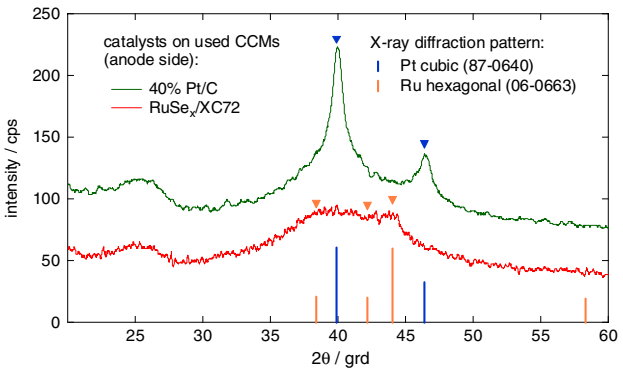

Fig. 15 X-ray diffraction spectra of electrochemically characterized catalyst layers as part of CCM with either Pt(40%)/C (—) or Ru(44.0 wt.%)Se(2.8 wt.%)/XC72 (—) catalyst

used and the pristine $RuSe_x$ catalysts feature no changes, the absence of any significant particle growth is deduced. This is in accordance with the observed stability in the DMFC durability tests.

For the platinum catalyst used a particle size of 8.9 nm was calculated from the Pt[111] Bragg reflex. If this value is compared with the mean diameter of 3.6 nm obtained from TEM analysis of the pristine platinum catalyst (see Sect. 3.2) it is obvious that the Pt particles experience significant coarsening by a factor of 2½, whereas the size of the $RuSe_x$ particles remains constant. This is further proof of stability of $RuSe_x$ catalysts and may be regarded as an advantage compared to platinum catalyst. However, in the future, the stability of $RuSe_x$ must be checked under more severe operating conditions, like dynamic operation (e.g. potential cycling).

4 Conclusions

$RuSe_x$ cathode catalysts were characterized as part of MEAs and CCMs. Under DMFC operating conditions these catalysts are methanol tolerant, selective for oxygen reduction and stable over a period of more than 1,000 h. MEAs with the best $RuSe_x$ catalyst (Ru(44.0 wt.%)-Se(2.8 wt.%)/VulcanXC72) achieve a maximum power density about 40% of the value obtained with commercial platinum cathode catalyst. However, there seems to be potential to improve the performance of $RuSe_x$ catalyst layers. This means on the one hand improvement of specific catalytic activity by modifying the surface composition of the $RuSe_x$ particles. On the other hand, the microstructure and properties of the catalyst layers and GDLs have to be further optimized. Electrochemical studies and structural investigations suggest that the following modifications may help to further improve performance: (i) increase in $RuSe_x$ fraction in the carbon

supported catalyst or even use of unsupported $RuSe_x$ catalyst, combined with increased $RuSe_x$ loading, (ii) more open structure/higher porosity of $RuSe_x$ catalyst layers, (iii) hydrophobization of carbon support, (iv) more homogeneous Nafion® distribution.

Acknowledgements We thank H. Schmitz for performing the aging experiments, S. Chirayath for preparation of MEAs, T. Wüst for CLSM analysis and E. Loveless for proof-reading. The financial support of the Ministry for Education, Research and Technology BMBF in the frame of the network "O2-RedNet" (contract number 03 SF 0302) is gratefully acknowledged. We thank German Academic Exchange Service DAAD for financial support of S. Kaytakoglu.

References

1. Tributsch H, Bron M, Hilgendorff M, Schulenburg H, Dorbandt I, Eyert V, Bogdanoff P, Fiechter S (2001) J Appl Electrochem 31:739
2. Bron M, Bogdanoff P, Fiechter S, Hilgendorff M, Radnik J, Dorbandt I, Schulenburg H, Tributsch H (2001) J Electroanal Chem 517:85
3. Hilgendorff M, Diesner K, Schulenburg H, Bogdanoff P, Bron M, Fiechter S (2002) J New Mater Electrochem Syst 5:71
4. Alonso-Vante N, Tributsch H, Solorza-Feria O (1995) Electrochim Acta 40:567
5. Neergat M, Leveratto D, Stimming U (2002) Fuel Cells: Fundam Syst 2:25
6. Scott K, Shukla AK, Jackson CL, Meuleman WRA (2004) J Power Sources 126:67
7. Schulenburg H, Hilgendorff M, Dorbandt I, Radnik J, Bogdanoff P, Fiechter S, Bron M, Tributsch H (2006) J Power Sources 155:47
8. Zehl G, Dorbandt I, Schmithals G, Radnik J, Wippermann K, Richter B, Bogdanoff P, Fiechter S (2006) ECS Transactions of the 210th ECS Meeting, Cancun, Proton Exchange Membrane Fuel Cells 6, in press
9. Bron M, Bogdanoff P, Fiechter S, Dorbandt I, Hilgendorff M, Schulenburg H, Tributsch H (2001) J Electroanal Chem 500:510
10. Marković N, Gasteiger HA, Ross PN (1995) J Phys Chem 99:3411
11. Khazova OA, Mikhailova AA, Skundin AM, Tuseeva EK, Havránek A, Wippermann K (2002) Fuel Cells: Fundam Syst 2(2):99
12. Kulikovsky AA, Schmitz H, Wippermann K, Mergel J, Fricke B, Sanders T, Sauer DU (2006) Electrochem Commun 8:754
13. David RL (eds) (1999) Handbook of chemistry and physics, 79th edn. CRC Press LLC, Boca Raton, Florida, pp 4–81, 4–82, 12–192 ISBN 0-8493-0479-2
14. Havránek A, Wippermann K (2004) J Electroanal Chem 567(2):305
15. Wippermann K, Klafki K (To be published)
16. Yu HM, Ziegler C, Oszcipok M, Zobel M, Hebling C (2006) Electrochim Acta 51:1199
17. David RL (eds) (1999) Handbook of chemistry and physics, 79th edn. CRC Press LLC, Boca Raton, Florida, pp 8–24 ISBN 0-8493-0479-2
18. Ralph TR, Hogarth MP (2002) Platinum Metals Rev 46(1):3
19. Rao V, Simonov PA, Savinova ER, Plaksin GV, Cherepanova SV, Kryukova GN, Stimming U (2005) J Power Sources 145:178
20. Uchida M, Fukuoka Y, Sugawara Y, Ohara H, Ohta A (1998) J Electrochem Soc 145:3708
21. Arico AS, Creti P, Antonucci PL, Cho J, Kim H, Antonucci V (1998) Electrochim Acta 43:3719
22. Havránek A, Klafki K, Mergel J, Schmitz H, Stolten D, Wippermann K (2003) In: Stolten D, Emonts B, Peters R (eds) Proceedings of the 2nd European Polymer Electrolyte Fuel Cell Forum, 30.6-4.7.2003, Luzern/Schweiz, European Fuel Cell Forum, Oberrohrdorf/Schweiz, ISBN 3-905592-13-4, p 623
23. Rheaume JM, Müller B, Schulze M (1998) J Power Sources 76:60
24. Bron M, Fiechter S, Bogdanoff P, Tributsch H (2002) Fuel Cells: Fundam Syst 2:137
25. Bron M, Radnik J, Fieber-Erdmann M, Bogdanoff P, Fiechter S (2002) J Electroanal Chem 535:113
26. LaConti AB, Hamdan M, McDonald RC (2003) In: Vielstich W, Gasteiger H, Lamm A (eds) Handbook of fuel cells-fundamentals, technology and applications, chapt. 49, vol 3. John Wiley & Sons, Chichester, U.K, p 647
27. Ferreira PJ, la O' GJ, Shao-Horn Y, Morgan D, Makharia R, Kocha S, Gasteiger HA (2005) J Electrochem Soc 152(11):A2256